中央研究院
資訊科學研究所
Institute of Information Science, Academia Sinica • Taipei, Taiwan, ROC

TR-IIS-17-004

Reactive human-aware wall following for indoor mobile robot

Chi-Wen Lo, Kun-Lin Wu, Chia-Wei Lin and Jing-Sin Liu

Dec. 08, 2017 (Revised) || Technical Report No. TR-IIS-17-004

http://www.iis.sinica.edu.tw/page/library/TechReport/tr2017/tr17.html

Reactive human-aware wall following for indoor mobile robot

Chi-Wen Lo* Kun-Lin Wu* Chia-Wei Lin* and Jing-Sin Liu*

Abstract

This paper describes the development of an indoor robotic surveillance system based on reactive wall following and human detection built on intelligent differential-drive mobile robot navigation. For this development of a surveillance mobile robot system that is assistive to human surveillance, we employ a commercially available wheeled mobile robot equipped with infrared sensors, sonar sensors and human detection sensors for perceiving the local indoor environment and detecting human presence. The system has two components: reactive wall following and human detection. The wall following is performed by a two-input (distances) single-output (heading angle) interval type-2 fuzzy logic system for heading direction control of a constant speed unicycle with online decision rules specifically designed for the task of stable right wall following. Proper reaction to the presence of an unexpected human is enabled in the wall-following course by human detection sensors. The design and implementation of an autonomous mobile robot human-aware surveillance system using reactive right wall following and human detection for two indoor surveillance tasks is demonstrated to work well in our lab testing.

Keywords

Wall following, reactive navigation, fuzzy logic controller, human detection, surveillance, patrol

Introduction

The incorporation of autonomous or human-shared autonomous mobile robots in the service of human living and as aids to office environments, agriculture, disaster management and manufacturing has been gaining more interest in recent years [18, 6]. Mobile robots have been deployed for numerous applications like mapping, home and health care, and search and rescue to support the safety and quality of life of people. Examples are cleaning floors and delivering goods such as medications to a specific location or area. Also, intelligent surveillance systems using one or a team of autonomous mobile robots are increasingly popular and useful in civil and military applications such as home or office building services, health care, and border patrol such as making security rounds in a factory.

A differential wheeled mobile robot is one of the most widely deployed indoor mobile robots [45]. Path following control is one of the major problems for wheeled mobile robots subject to nonholonomic rolling without slipping constraints [34, 35, 36]. Wall/boundary following, i.e. moving along the boundary (or along a direction parallel to the boundary tangent), generally modeled as a smooth planar curve, at a safe distance could be a basic behavior of more complex navigation behaviors for finishing various autonomous tasks in an *a priori* unknown environment or could be used for map-building applications, since following the wall could reduce the odometry errors by exploiting the straightness or tangent of the wall. Wall following or border patrolling viewed as a variation of path following is a biologically inspired, sensor-based robust navigation or control strategy (specifically, path following/tracking) commonly used by bugs and for reactive nonholonomic mobile robot navigation (see [1], [2], [4], [7] ,[12], [15], [16], [19], [25]-[28], [30]-[34], [39] among a large literature). Computational intelligence-based approaches such as neural networks [26], [39], evolutionary algorithms [15], and fuzzy systems [20], [25], [43] and dynamical systems approaches such as Lyapunov stability-based [7], [16], [32], [34] or chaotic-based [12] approaches are developed for the boundary following control problem in the aforementioned works. Wall following is integrated with the potential field-based navigation to help escape the local minima (navigation limit cycle) associated with potential fields [30]. Wall following could be used to avoid obstacles during path following [9]. However, some complications in the indoor environment could cause a fixed wall-following algorithm without switching to fail [13]. [32] proposed that fuzzy logic or switching among an ensemble of behavior controllers is the trend for wall-following control.

Uncertainties in both sensor readings and world modeling are ubiquitous in real-world navigation of a wheeled mobile robot that is a nonlinear system with nonlinearities arising from the motor drive and kinematics of motion due to the nonholonomic constraints. The uncertainty and nonlinearity cause technical difficulty and unpredictability for navigating a nonholonomic wheeled mobile robot in the realization of path following tasks in the real world [41]. To cope with the disturbances and uncertainties that are stochastic in nature, one solution framework is partially observable Markov decision processes (POMDP) [38] to generate plans that are robust to uncertainty. Another approach is designing additional compensators cascaded with the primary navigation controllers [37]. On the other hand, fuzzy logic theory has been widely applied to the design of intelligent controllers for uncertain systems. Designing a controller based on informative control decisions provided by fuzzy logic has been demonstrated via simulations and real-world experiments

* *Institute of Information Science, Academia Sinica Nangang, Taipei, Taiwan 11529, ROC*
Corresponding author:liu@iis.sinica.edu.tw

to be a popular and useful method for improving the performance of mobile robot reactive navigation and control [8], [15], [20], [22], [25], [30]-[31]. The advantages of using fuzzy logic for intelligent control are as follows: 1) It does not need a detailed or precise physical or mathematical model of the plant derived from first principles, and thus can simplify the control design process of an unknown complex, nonlinear and time-varying system such as a robot; 2) Control rules that can incorporate expert knowledge or experience are more flexible and transparent. They replace mathematical values in describing a control system by using linguistically ambiguous expressions for designing controllers that are able to deliver satisfactory performance in the face of uncertainty and imprecision; 3) The controller can efficiently implement the basic rules that emulate expert decision making and is easy to debug. Fuzzy logic is thus well suited for real mobile robot navigation, where correct reactive behaviors could be inferred and generated based on the real-time sensing of an uncertain, unstructured and complex environment. To avoid large and unpredictable motions that are closely related to high control energy, the performance of a type-2 fuzzy system is generally smoother than a type-1 fuzzy system [22], in particular for wall following [15], in which the antecedent in each fuzzy rule uses a type-2 fuzzy set to enhance the robustness.

In typical indoor environments, the presence of humans is inevitable and often unpredictable. The humans can be viewed by the robot as moving obstacles, social agents not to be disturbed, or intruders, or as partners in joint motion with particular interests [18]. Therefore, the presence of humans in a robot workspace that causes a situation of spatial conflict adds a new dimension to the navigation of a mobile robot. It is important for the robot to take into consideration the presence of humans in executing tasks and to decide on-line how to react it. This presents many challenging technical problems, among which are the reliable and effective detection of human presence for the safety of both robot and human, and the enabling of better human-robot interaction for the completion of robot missions. Human detection was studied in [10], [11], [24]. Here we consider a situation in which an unexpected person appears instantaneously on the wall-following route. In our work, the robot is equipped with human detection sensors so that it could be used in an indoor environment to detect the presence of humans near the robot. The technique is novel for human-aware robotic navigation. We present a surveillance system based on an interval type-2 fuzzy reactive wall-following mobile robot with the detection of human appearance in an indoor environment.

This paper is organized as follows. In “The Mobile Robot” section, we present the mobile robot platform and its unicycle kinematics. The “Sensors” section introduces the sensors embedded on the mobile robot used for wall following and human detection. The “Intelligent Control Structure” section presents the interval type-2 fuzzy controller structure including the analysis and design of wall-following rules. “Event-based Practical Stability Analysis” shows that the robot takes a series of actions based on the fuzzy rules in each encountered situation around the equilibrium that corresponds to the stable wall-following behavior that could make the robot recover from the deviation from the parallelism to the wall. Experimental results of two indoor navigation tests are reported to demonstrate wall following with human detection in the section “Experimental Results and Discussions”. Conclusions are made in the section “Conclusions”.

The mobile robot

A mobile robot consists of a mechanical system, on-line boundary and obstacle detection provided by the embedded sensors, and communication and control components.

Wheeled mobile robot

For the development of intelligent right wall following, we selected the mobile robot X80 from Dr. Robot Inc. as the mobile robot platform on which to develop, design and test our intelligent control algorithm for boundary surveillance.

The X80 is a differential-drive robot which has two independently controlled wheels with one on each side, and a passive wheel for stability. Fig. 1(a) shows the physical and sensor configurations, and Fig. 1(b) is a photo of the mobile robot X80. The sensors consist of three groups - sonar sensors on the front, left front and right front; an infrared (IR) sensor on the right; and two human detection sensors, one on each side of the wheels.

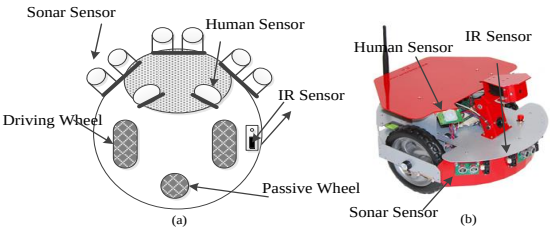

Fig. 1. The mobile robot platform X80 for right wall following. (a) The sensor configuration, (b) The photo.

Table 1 The Robot X80 parameter values

Robot Parameter	Value
Wheel Radius (r)	12.5(cm)
Distance Between Two Wheels (d)	25(cm)
Dimensions	38(cm) ×25.5(cm)
Weight	3.5kg
Max Speed	1m/sec
Max. Angular velocity	0.75 (rad/s)
Torque	300(oz.-inch)
Curvature constraint	1.5 (1/m)

Drive system

The X80 robot is an integrated electronic and software robotic system, and provides a set of ActiveX control components (SDK) developed for C, Matlab and LabVIEW that are available to the designer. The robot offers full WiFi (802.11b) and uses a wide range of sensors including an IR sensor, sonar sensors, and human detection sensors (detailed in later sections) for surveillance applications. The motion of the

mobile robot is controlled by two independent DC motors for two wheels with an incremental encoder via the controlling output signal of the H-Bridge by Pulse Width Modulation (PWM), where the differential velocity is coordinated to drive in the desired moving direction such as forward or rotation. The coordinate frame of the robot motion is shown in Fig. 2, where the robot coordinate is defined in the middle of the driving wheels.

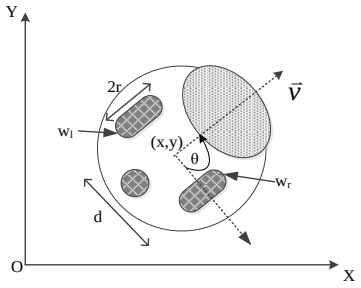

Fig.2. The global (earth) and robot coordinate systems for mobile robot motion

Given the robot parameters listed in Table 1, we consider the transformation from wheel rotational velocities to robot linear and rotational velocities can be expressed as follows:

$$\begin{bmatrix} v \\ \omega \end{bmatrix} = \begin{bmatrix} \frac{r}{2} & \frac{r}{2} \\ -\frac{r}{d} & \frac{r}{d} \end{bmatrix} \begin{bmatrix} \dot{q}_{left} \\ \dot{q}_{right} \end{bmatrix}$$

where q_{left} and q_{right} denote initial left and right wheel angular rotation, respectively, and $w_r = \dot{q}_{right}, w_l = \dot{q}_{left}$ are their angular velocities; r is wheel radius; d is the width of the vehicle (i.e. the distance between two driving wheels), and $v = \sqrt{\dot{x}^2 + \dot{y}^2}$ and ω denote the (desired) linear (i.e. forward, driving) velocity and angular (i.e. steering) velocity of the robot, respectively. The kinematic model of the mobile robot using the wheel angular velocity $\dot{q}_{left}$ and $\dot{q}_{right}$ as input can thus be described as follows

$$\begin{cases} \dot{x} = v\cos\theta = \frac{r}{2}(\dot{q}_{left} + \dot{q}_{right})\cos\theta \\ \dot{y} = v\sin\theta = \frac{r}{2}(\dot{q}_{left} + \dot{q}_{right})\sin\theta \\ \dot{\theta} = \omega = \frac{r}{2d}(\dot{q}_{left} - \dot{q}_{right}) \\ \kappa = \omega / v \end{cases} \quad (1)$$

where $\omega \le \omega_{\max}$, $v \le v_{\max}$, and κ is the curvature with the constraint $|\kappa| \le \kappa_{\max}$, $\kappa_{\max}$ is the maximal curvature of the path. The turning angle θ (the output from fuzzy controller detailed later) determines the actual speed commands applied to each wheel of the robot corresponding to $\dot{q}_{right}, \dot{q}_{left}$ as follows:

$$V_{Right} = (d/2) * \frac{\theta}{180} * \pi + \dot{q}_{right} \quad (2)$$

$$V_{Left} = (d/2) * \frac{\theta}{180} * \pi - \dot{q}_{left} \quad (3)$$

The right and left wheel speeds derived from the angular and linear velocities of the robot are the reference input to drive the robot. It is well known that the unicycle (1), viewed as an (underactuated) non-reversible nonlinear dynamic system without drift, is controllable, i.e. given two arbitrary configurations, there exists a path linking them with the associated wheel speed inputs.
Differentiating (1), we obtain

$$\frac{d^2}{dt^2}\begin{pmatrix} x \\ y \\ \theta \end{pmatrix} = \begin{pmatrix} -\kappa\sin\theta \\ \kappa\cos\theta \\ \dot{\kappa} \end{pmatrix} v^2 + \begin{pmatrix} \cos\theta \\ \sin\theta \\ \kappa \end{pmatrix} \dot{v}$$

Suppose that the unicycle moves with constant linear speed, and its path is composed by the constant curvature segments (such as straight lines and circular arcs), then $\dot{\kappa} = 0$, and $\dot{v} = 0$. Then the above equation for acceleration becomes

$$\frac{d^2}{dt^2}\begin{pmatrix} x \\ y \\ \theta \end{pmatrix} = \begin{pmatrix} -\sin\theta \\ \cos\theta \\ 0 \end{pmatrix} \kappa v^2$$

with the heading θ and normal acceleration κv^2 as the input. A straight-line forward motion is performed by commanding the same velocity to left and right wheels. Rotation is defined as follows: left turn (positive θ) denotes counterclockwise rotation; right turn (negative θ) denotes clockwise rotation). It is noted here that the unicycle model considered in this paper allows turning about its axis on the spot, which corresponds to $\sqrt{x^2 + y^2}$ is a constant, $v = 0$, and θ rotates an angle θ_d, by commanding the same left and right wheel speeds but in opposite directions. A circular path of radius *R* corresponds to a constant linear and angular velocity input

$$v = v_d, \omega = v_d / R$$

where v_d is the desired linear speed. These two primitive motions are very convenient for a wall following task that

requires the robot to rotate to a desired heading angle then move forward. A block diagram of generating steering velocities of rotational and translational motions enabling a differential-drive mobile robot to produce the basic motions such as a straight-line motion, a circular motion within the maximum curvature constraint, or a non-zero rotation on the spot that are compatible with the kinematics of the mobile robot is depicted in Fig. 3.

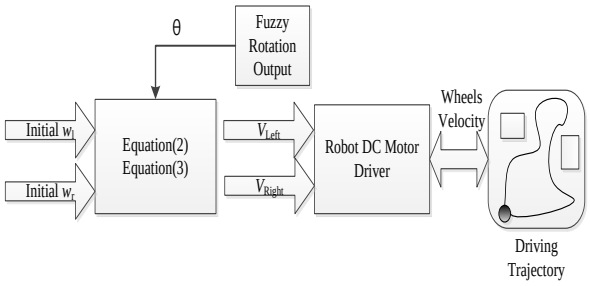

Fig. 3. Block diagram of generating wheel velocities for wheeled mobile robot. Each wheel is actuated directly from a fuzzy controller output heading angle compatible with the mobile robot kinematics. Then equations (2) and (3) compute the control signal for the wheel motors that move the robot modelled as a unicycle.

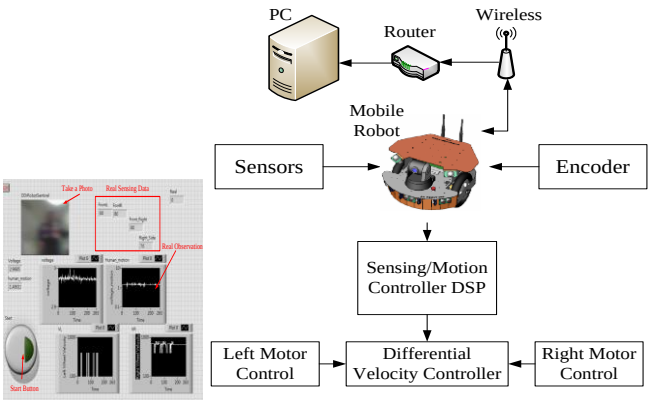

Fig.4. Wireless control system with Labview GUI (left photo) on the remote computer to control the mobile robot.

Fig. 4 shows the structure of the robot control system through wireless communication, which the navigation algorithm runs directly on the remote PC. Via a serial wireless module, velocity commands to the mobile robot are received from the remote PC, while the results of the sensing from current robot location are transmitted to the remote PC. A Labview graphical user interface (GUI) on the PC at the user's end is designed for real-time monitoring, control and sensor data management.

Sensors

During wall following, the state of the environment could be dynamically changing. Previous work shows that a wall-following robot could complete its mission with the assistance of various sensors: tactile sensors [19], cost-effective low-level (noisy and low-resolution) range sensors such as ultrasonic (sonar) [1, 4, 5, 7, 28, 33] and infrared (IR) [16] sensors, and laser range finders [21], which provide the required range and/or bearing information to the wall in the directions at which they are pointing in space. To support the sensory requirement of an indoor mobile robot surveillance system based on wall following, a multisensory system composed by three types of sensors, i.e. cost-effective proximity sensors (ultrasonic and infrared sensors) to measure the distance of robot from the wall or obstacles within the sensing range and human detection sensors to detect the presence of humans in their fields of view, is embedded in the mobile robot X80.

Range sensors

1. Ultrasonic sensors

Ultrasonic sensors have been commonly used for mobile robot navigation purposes owing to their accurate range measurements, robustness and low cost [3]. They have been used in mobile robot localization [23] and to achieve obstacle avoidance and wall following [1, 4, 5, 7, 29]. The DUR5200 ultrasonic sensor can measure a distance range from 10 to 340cm. The sound wave propagation speed v can be calculated by the following formula (4):

$$v = 331.5 + 0.6 \cdot T[m/\sec] \quad (4)$$

where T is the air temperature $(^{\circ}C)$. The time interval t_d between the instant when the measurement is enabled and the instant when the echo signal is received is calculated by count value (0~255) and count cycles of 80 us times as follows (5):

$$t_d = count \cdot count\_rate \quad (5)$$

The distance to object (in meters) within the detectable area can be estimated by the time taken to receive an echo signal by the sensor:

$$\text{distance to the object} = (t_d * v)/2 \quad (6)$$

2. Infrared proximity sensors

Infrared (IR) sensors are based on emission and reception of infrared light. The GP2Y0A21YK Sharp IR sensor that detects an object within a distance range from 10 to 80cm has an analog output that varies from 3.1V at 10cm to 0.4V at 80cm, which is suitable for indoor applications.

Human detection sensors [14]

In a real indoor environment, objects, including pets and humans, may appear abruptly. These living objects generate heat and also generate infrared radiation. A person who comes close to the mobile robot appears as an unexpected close-in obstacle to the robot. The human detection sensors in charge of the presence of humans provide reliable and effective

detection of the unexpected appearance of humans in the vicinity of the mobile robot. Two human detection sensors are mounted on the X80 mobile robot, one on the left side and one on the right (as depicted in Fig. 1). Fig. 5 illustrates the detection of the presence or absence of a human in the vicinity of the mobile robot using the human detection sensor, which is able to detect human presence in a range up to 500 cm. The dimensional drawing and horizontal view pattern are shown in Fig. 6. There are analog outputs returned when no human is present on the route, in which case the output voltage of the human sensor is 1.5V. The output voltage fluctuates between 0 and 3V. Therefore, we can set a threshold for feedback voltage of the human detection sensor to continuously detect whether there is an appearance of a person in the way of wall following to avoid an imminent collision and keep both the vehicle and the human safe.

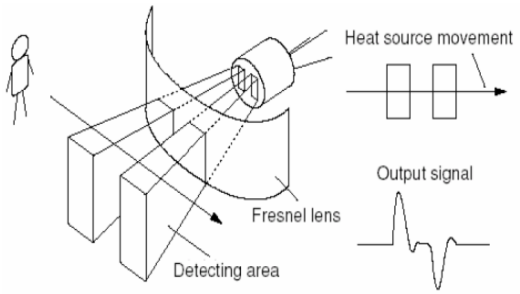

Fig. 5. Detection of human presence using heat [14].

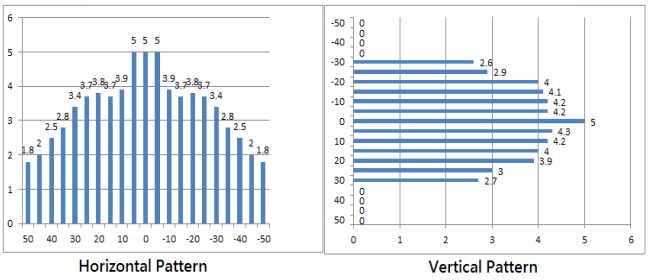

Fig. 6. The horizontal and vertical view patterns of the human detection sensor shows the horizontal angular scan range $[-50^0, 50^0]$ and the vertical angular scan range $[-30^0, 30^0]$, with a maximum front sensing range of 5m.

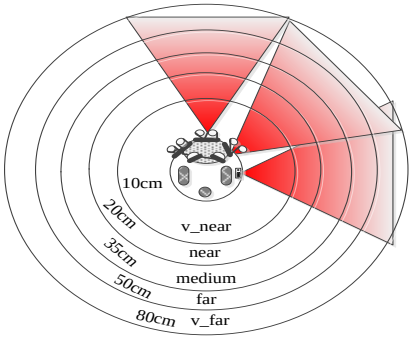

Fig. 7. The partition of sensing range of the sensors into five circular envelopes of increasing radius to cover the detectable area. The figure shows three sensors for right, front right and front sensing for right wall following. These are represented as fuzzy membership functions.

Table 2. 25 rules for right wall following with two inputs (front right distance and right distance to the wall) and one output (heading) (v_ denotes very)

	IF/input		THEN/output
	Front Right	Right	Heading ($\delta\theta$)
Rule 1	v_near	v_near	v_Left
Rule 2	v_near	near	v_Left
Rule 3	v_near	medium	v_Left
Rule 4	v_near	far	v_Left
Rule 5	v_near	v_far	Left
Rule 6	near	v_near	v_Left
Rule 7	near	near	v_Left
Rule 8	near	medium	v_Left
Rule 9	near	far	v_Left
Rule 10	near	v_far	Left
Rule 11	medium	v_near	Medium
Rule 12	medium	near	Medium
Rule 13	medium	medium	Medium
Rule 14	medium	far	Medium
Rule 15	medium	v_far	Medium
Rule 16	far	v_near	Right
Rule 17	far	near	Right
Rule 18	far	medium	Medium
Rule 19	far	far	Right
Rule 20	far	v_far	Right
Rule 21	v_far	v_near	Right
Rule 22	v_far	near	Right
Rule 23	v_far	medium	Medium
Rule 24	v_far	far	Right
Rule 25	v_far	v_far	Right

Intelligent controller structure

Based on relative acceleration dynamics in polar coordinates, [17] formally derived that the heading angle is the key control of wall-following behavior considered as a special case of obstacle avoidance behavior. Thus our control objective of right wall following is to derive an appropriate heading angle for the mobile robot and to maintain a safe distance to the wall [4], [16], where the turning around the corner or deadend is the most difficult part since at least two walls are sensed in these situations. In this paper, a design of an interval type type-2 fuzzy logic controller for a wall-following mobile robot is presented. Our wall-following control is a behavior-based differential velocity control algorithm that allows the mobile robot to operate at reduced energy consumption, where the mapping between the local information of the state of the environment obtained from the sensors and the reactive behaviors of the mobile robot heading is defined by the rules for wall-following situations that simulate the experience of human control.

Concrete Rules design

We consider a unicycle mobile robot (1) that moves with constant speed and is controlled by its angular velocity driven by an interval type-2 fuzzy heading control. For the design of fuzzy reactive behavior-based control, a proper partition of input and output and design of decision rules for determine proper actions are required. The robot has a large state-action space for finishing a variety of tasks. Hence a rule is defined as "performing an action a in configuration q takes the robot to a new configuration q_a ". Formally, we define the perception-action mapping from the robot current state to the

executable action that the robot (1) can achieve based on on-line sensor feedback. For the wheeled mobile robot X80 and the task of right wall following represented by an ordered sequence of actions, the sensing range of sensors located at the front, front right, and right sides is partitioned accordingly into the front, front right, and right distances as shown in Fig. 7 to sense the surrounding environment. The distance for each sensing direction is classified as five circular envelopes of increasing radius which are named v_near, near, medium, far, and v_far to identify the distance to the wall. Note that for each range sensor only the half-circle in front of the mobile robot is the sensing range. The output is the incremental heading angle (θ). These are represented as fuzzy membership functions (see the subsection "Variation of Interval Type-2 Membership Functions").

The line feature of the wall is robust to the orientation of sensors and the environmental conditions, and thus is suitable for the task of path following. From the view of local path planning and following, the task of wall following is that a mobile robot is required to move forward along a path that is defined as parallel to (tangent to) the wall without specifying an explicit goal. When restricted to right wall following, the behavior set of the robot (1) in different situations is defined in Table 2 derived from the perception capability of identifying the situations encountered by the mobile robot during wall following and task-directed actions to guide the robot towards the next intermediate position. Table 2 is composed by 25 rules that are easy to understand and to implement in real time. The controller maps from the robot state corresponding to the front right and right distances of the robot from the walls to the heading angle, whose four directions are v_left, left, medium, and right.

The sensors that the robot relies on to gather local information on the surrounding environment are prone to errors. For example, the ultrasonic sensor has the problem of intrinsic angular uncertainty, echoes, and multiple-reflections-related misreadings [3]. In order to describe the effects of uncertainty due to the accuracy and resolution of different types of sensors and to a number of measurements contaminated with various types of noise and errors, the partition of ranges could be represented by fuzzy membership functions. It is generally accepted that type-2 fuzzy logic possesses better capability of handling uncertainties [8, 22]. In what follows, we introduce the type-2 fuzzy logic system employed here as the basis of planning, control, and decision making of an intelligent wall-following mobile robot.

Type-2 fuzzy logic system

A type-2 fuzzy set $\tilde{A}$ is characterized by the three-dimensional membership function as (7).

$$\tilde{A} = \{((\mathbf{x}, u), \mu_{\tilde{A}}(\mathbf{x}, u)) \mid \forall \mathbf{x} \in X, \forall u \in J_{\mathbf{x}} \subseteq [0,1]\} \quad (7)$$

where X is the universe of the primary variable $\mathbf{x}$ of $\tilde{A}$, u is called the secondary variable and has a domain $J_{\mathbf{x}} \subseteq [0,1]$

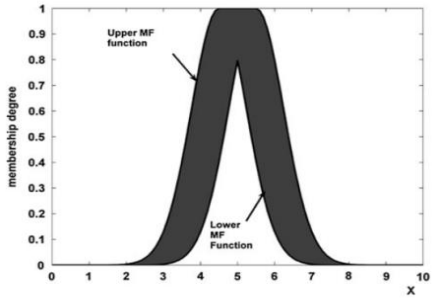

Fig. 8. Interval type-2 membership function showing the upper and lower bounds of uncertainties with upper and lower membership functions, with the shaded area being the FOU [8].

at each $\mathbf{x}$. $J_{\mathbf{x}}$ is called the primary membership of $\mathbf{x}$. For $\mathbf{x}' \in X$ and $\forall u \in J_{\mathbf{x}'} \subseteq [0,1]$, there is a vertical slice of $\mu_{\tilde{A}}(\mathbf{x}, u)$, a type-1 fuzzy set

$$\mu_{\tilde{A}}(\mathbf{x} = \mathbf{x}', u) \equiv \mu_{\tilde{A}}(\mathbf{x}') = \int_{u \in J_{\mathbf{x}'}} 1/u, J_{\mathbf{x}'} \subseteq [0,1]$$

called a secondary membership which defines the possibilities of primary membership, where $\int$ denotes the union over all admissible $u \in J_{\mathbf{x}'}$. When $\mu_{\tilde{A}}(\mathbf{x}, u) = 1, \forall \mathbf{x} \in X, \forall u \in J_{\mathbf{x}} \subseteq [0,1]$, we have an interval type-2 membership function [22]. As shown in Fig. 8 [8], an interval-valued fuzzy set $\tilde{A}$ is defined by its upper membership function $\bar{\mu}_{\tilde{A}}(\mathbf{x})$ and lower membership function $\underline{\mu}_{\tilde{A}}(\mathbf{x})$, $\forall \mathbf{x} \in X$, therefore an interval type-2 set can be seen as an uncountable number of type-1 sets. The uncertainty in the primary memberships of an interval type-2 fuzzy set $\tilde{A}$ is completely represented by the area between upper and lower membership functions, which is called the footprint of uncertainty (FOU) defined as

$$\mathrm{FOU}(\tilde{A}) = \bigcup_{\mathbf{x} \in X} J_{\mathbf{x}}.$$

Thus for interval type-2 fuzzy set

$$\mathrm{FOU}(\tilde{A}) = [\underline{\mu}_{\tilde{A}}(\mathbf{x}), \bar{\mu}_{\tilde{A}}(\mathbf{x})], \forall \mathbf{x} \in X,$$

the FOU contains infinitely many functions that fill the area between upper and lower membership functions. Any membership functions within the FOU can be reconstructed by the lower and upper membership functions.

The type-2 fuzzy logic system is shown in Fig.10. It includes a fuzzifier, a rule base, a fuzzy inference, a type reducer and a defuzzifier. Defuzzification of a type-2 fuzzy set may be considered a two-stage process: The output processing to

produce a crisp output y is performed by the sequential operation of a type reducer and a defuzzifier. For our purpose of wall-following control design, we consider a type-2 fuzzy

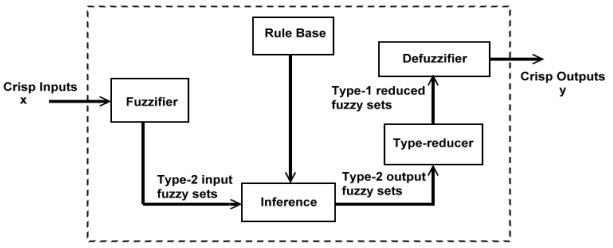

Fig.9 A Type-2 fuzzy logic system. The fuzzy input can be either a type-1 or a type-2 fuzzy set (shown in this figure).

logic system with p inputs (linguistic variables) $x_1 \in X_1, \ldots, x_p \in X_p$ and one output $y \in Y$.

1) Fuzzifier: The fuzzifier maps a numeric $p-$ vector $\mathbf{x} = (x_1, \ldots, x_p)^T \in X$ into a type-2 fuzzy set $\tilde{A}_{\mathbf{x}}$ in X, an interval type-2 fuzzy set in our case.

2) Rules: Assume there are *M* (25 in this paper) rules of which the antecedents are interval type-2 sets, and the consequent is a crisp number. The *l*th rule can be written as a multi-input single-output rule

$$R^l: If\ x_1 is \tilde{F}_1^{\,l}\ and \cdots and\ x_p is \tilde{F}_p^{\,l},\ Then\ y is \tilde{G}^l, l = 1, \ldots, M \quad (8)$$

where the antecedents $\tilde{F}_i^{\,l}$ and consequents $\tilde{G}^l$, $i = 1, \cdots, p$, $l = 1, \ldots, M$ are appropriate interval type-2 fuzzy sets for each rule.

3) Inference: Inference is a mapping from fuzzy input sets to fuzzy output sets. Let the Cartesian product $\tilde{F}_1^{\,l} \times \cdots \times \tilde{F}_p^{\,l} = \tilde{A}^l$. R^l can be rewritten as a fuzzy implication (9).

$$R^l: \tilde{F}_1^{\,l} \times \cdots \times \tilde{F}_p^{\,l} = \tilde{A}^l \to \tilde{G}^l, l = 1, \ldots, M \quad (9)$$

R^l is described by the membership function $\mu_{R^l}(\mathbf{x}, y) = \mu_{\tilde{A}^l \to \tilde{G}^l}(\mathbf{x}, y)$, where

$$\begin{aligned} \mu_{R^l}(\mathbf{x}, y) &= \mu_{\tilde{A}^l \to \tilde{G}^l}(\mathbf{x}, y) \\ &= \mu_{\tilde{F}^l}(x_1) \bigcap \cdots \bigcap \mu_{\tilde{F}_p^{\,l}}(x_p) \bigcap \mu_{\tilde{G}^l}(y) \\ &= [\bigcap_{i=1}^p \mu_{\tilde{F}_i^l}(x_i)] \bigcap \mu_{\tilde{G}^l}(y) \end{aligned} \quad (10)$$

where $\bigcap$ is the intersection under product t-norm so that for two type-1 fuzzy sets *A* and *B* described by their membership functions $\mu_A(\mathbf{x}), \mu_B(\mathbf{x})$

$$\mu_{A \cap B}(\mathbf{x}) = \min\{\mu_A(\mathbf{x}), \mu_B(\mathbf{x})\}, \forall \mathbf{x} \in X$$

The intersection of two interval type-2 fuzzy sets $\tilde{A}, \tilde{B}$ is defined as

$$\mu_{\tilde{A} \cap \tilde{B}}(\mathbf{x}) = 1/[\underline{\mu}_{\tilde{A}}(\mathbf{x}) \wedge \underline{\mu}_{\tilde{B}}(\mathbf{x}), \overline{\mu}_{\tilde{A}}(\mathbf{x}) \wedge \overline{\mu}_{\tilde{B}}(\mathbf{x})], \forall \mathbf{x} \in X$$

Then the firing set $\bigcap_{i=1}^p \mu_{\tilde{F}_i}(x_i' \equiv F^l(\mathbf{x}'))$ is an interval type-1 set described as follows

$$F^l(\mathbf{x}') = [\underline{f}^{\,l}(\mathbf{x}'), \overline{f}^{\,l}(\mathbf{x}')] \quad (11)$$

where $\underline{f}^{\,l}(\mathbf{x}') = \underline{\mu}_{\tilde{F}_1^l}(x_1') * \cdots * \underline{\mu}_{\tilde{F}_p^{\,l}}(x_p')$ (12)

and $\overline{f}^{\,l}(\mathbf{x}') = \overline{\mu}_{\tilde{F}_1^l}(x_1') * \cdots * \overline{\mu}_{\tilde{F}_p^{\,l}}(x_p')$ (13)

where * is the product t-norm (i.e. intersection) operation.

4) Type Reducer: A type reducer produces a type-reduced set, a type-1 fuzzy set that is a fuzzy representation of the centroid of the type-2 fuzzy set. This type-1 fuzzy set is also an interval set. A popular type reduction method is to compute the centroid of an IT2 FS. We use center-of-sets (cos) typereduction, which is expressed as an interval type-1 set (14) determined by the left and right end points y_l and y_r

$$\begin{aligned} Y_{\cos}(\mathbf{x}) &= [y_l, y_r] \\ &= \int_{y^l \in [y_l^{\,1}, y_r^{\,1}]} \cdots \int_{y^M \in [y_l^{\,M}, y_r^{\,M}]} \cdots \\ &\int_{f^1 \in [\underline{f}^1, \overline{f}^1]} \cdots \int_{f^M \in [\underline{f}^M, \overline{f}^M]} 1 / \frac{\sum_{i=1}^M f^i y^i}{\sum_{i=1}^M f^i} \end{aligned} \quad (14)$$

Here the integral sign denotes the collection of all points with associated membership functions. The interval set corresponds to the centroid of the type-2 interval consequents $\tilde{G}^i$

$$C_{\tilde{G}^i} = \int_{\theta_1 \in J_{y_1}} \cdots \int_{\theta_N \in J_{y_N}} 1 / \frac{\sum_{i=1}^N y_i \theta_i}{\sum_{i=1}^N \theta_i} = [y_l^i, y_r^i] \quad (15)$$

The values of y_l and y_r define the output interval of a type-2 fuzzy system, as equations (16) and (17).

$$y_l = \frac{\sum_{i=1}^M f_l^{\,i} y_l^i}{\sum_{i=1}^M f_l^{\,i}} \quad (16)$$

$$y_r = \frac{\sum_{i=1}^{M} f_l^{\,i} y_r^{i}}{\sum_{i=1}^{M} f_l^{\,i}} \tag{17}$$

5) Defuzzifier: $Y_{\cos}(\mathbf{x})$ is then converted to a crisp output through the defuzzifier. The defuzzified output of an interval type-2 fuzzy logic system is the average of y_l, y_r of the interval set $Y_{\cos}(\mathbf{x})$

$$y(\mathbf{x}) = \frac{1}{2}(y_l(\mathbf{x}) + y_r(\mathbf{x})) \tag{18}$$

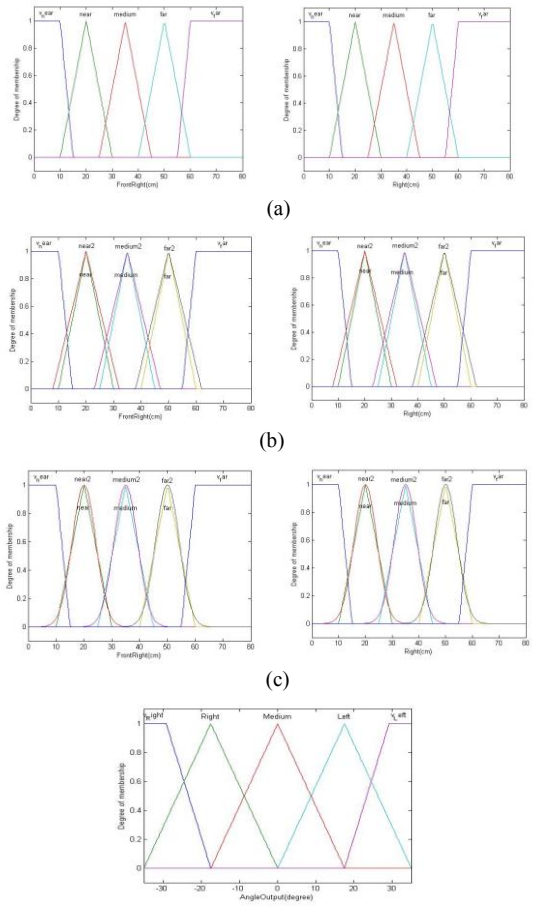

Fig.10 Membership functions. (a) traditional type-1 (one triangular), (b) type-2 (two triangular), (c) variation type-2 (one triangular and one Gaussian) input membership functions, and (d) traditional type-1 (one triangular) output membership function.

Variation of interval type-2 membership functions

The input distance in the range [0,80]cm is mapped to five fuzzy sets (representing v_near, near, medium, far, and v_far), while the output heading angle in the range [-35, 35]degrees (negative sign and positive sign represent clockwise and counterclockwise rotation, respectively) is mapped to five type-1 triangular fuzzy sets (representing v_right, right, medium, left, and v_left). To deal with uncertainties of real range sensing data input, two types of symmetrical membership functions of equal spread are studied: triangular and Gaussian. The triangular membership function has zero value at the boundaries of domain, while the Gaussian membership function is smooth and non-zero for every point in the domain. We propose to use a variation of type-2 fuzzy membership functions in which the upper and lower membership functions that define the FOU of an interval type-2 fuzzy set have two different function types: one is triangular type and the other is Gaussian type. Fig. 10 shows the membership functions in which Fig. 10(a), (b), (c) and (d) are traditional type-1 triangular, interval type-2 triangular, and variation interval type-2 (one triangular and one Gaussian) membership functions of designed inputs, and a designed output membership function, respectively.

A preliminary simulation revealing the performance of three types of the fuzzy logic system is shown in Fig. 11 where Fig. 11(a) is traditional (type-1), Fig. 11(b) is interval type-2, and Fig. 11(c) is a variation interval type-2 fuzzy logic system, respectively. There are two inputs to the fuzzy controller and one output. The two inputs are right and front right distances to the wall, where each of them has two (upper and lower) membership functions, and for the task of wall following, the front sensor which points in the forward direction of the robot is used to detect the need for turning around the corner. The output is the change of attitude. The main thing we observe from Fig. 11 is that applying variation interval type-2 fuzzy system causes a more balanced control surface.

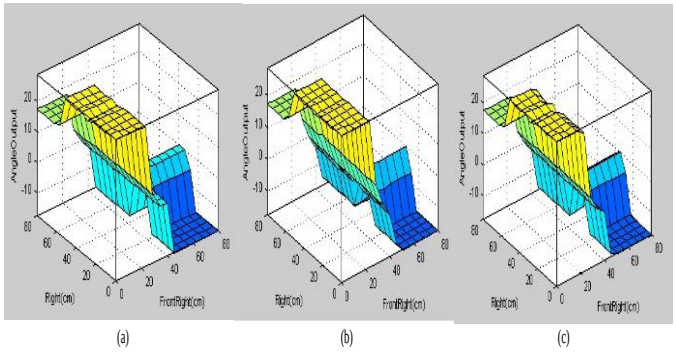

Fig. 11. Control surface of the simulation with (a) traditional type-1 (one triangular membership function), (b) interval type-2 (two triangular membership functions), (c) variation interval type-2 (one triangular membership function and one Gaussian membership function) fuzzy system with two inputs and one output task in an indoor environment.

Situations of wall following for fuzzy rules design

The robot is assumed to move at a constant forward speed. The only requirement for the sensory system for a robot following the walls in a simply connected environment with corners or following the contour of an obstacle is that a segment of the wall or of the contour of the obstacle can be perceived by one or more sensors, and at least one sensor can perceive one or more walls or segments during the robot's motion, or the robot can recover from the loss of wall situation. Once perceiving the state of the wall, including the distance to and orientation of the walls, the robot should identify the situation it faces and at the same time perform local path planning to turn an angle according to the sensory

information received, which is implemented via fuzzy decision rules in this paper, to determine the movement direction in the presence of measurement errors in heading. For our working system X80 shown in Fig. 1, the sensory information provided by three distance sensors on each side (left or right) of the mobile robot is used to correctly identify the situation the robot faces and the wall discontinuities (i.e. corners and deadends). The robot could follow a wall on its right (or left) when the detected wall is to the right (or left) of the robot. In what follows, we consider only right-wall following. We assume that the wall could be well represented by line segments. As the mobile robot moves and senses one or more segments of the wall or the obstacle contour, three primary situations (depicted in Fig. 12, Fig. 13 and Fig. 14) are distinguished for on-line wall following rules design (with reference to prior work [1], [9], [32], [33] among others) summarized in Table 3:

(i) First situation. Detection of a flat wall or a smooth wall shown in Fig. 12. This situation is recognized by the robot when right and front right sensors detect a wall without any frontal detection.

(ii) Second situation. Detection of a sharp corner shown in Fig. 13.

(iii) Third situation. Detection of a dead end shown in Fig. 14.

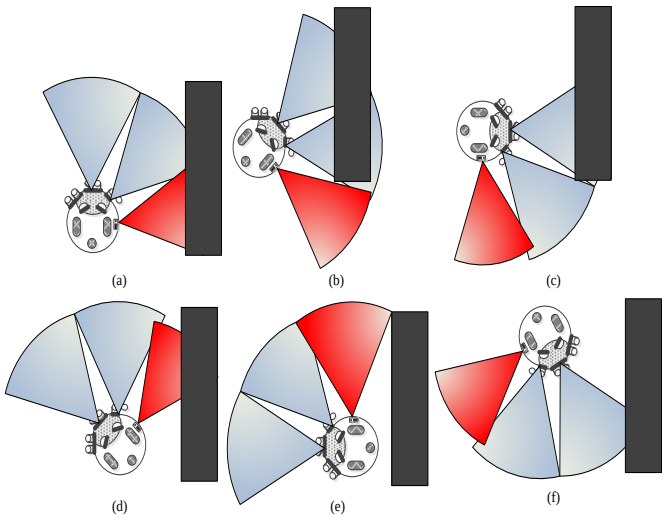

Fig. 12. First situation. The flat wall relative to the mobile robot is encountered in six situations (with reference to Table 2 and Table 3).

(a) Nominal situation. Parallel to the wall; it is handled by rules 11~15 with medium output heading angle, where the desired motion is to move straight.

(b) Front right and right sensors detect approaching the wall; rules 1~10 handle the situation; the output action is to turn left (left or v_Left).

(c) Front sensors detect approaching the wall; the action is rotation on the spot until the front is clear of the wall.

(d) Front right and right sensors detect the deviation from the wall; rules 16~23 handle the situation, and the desired action is to turn right to approach the wall.

(e) & (f) are the situations of losing the wall; rules 24 & 25 handle the situation, and the desired movement is to turn right slightly to look for a wall.

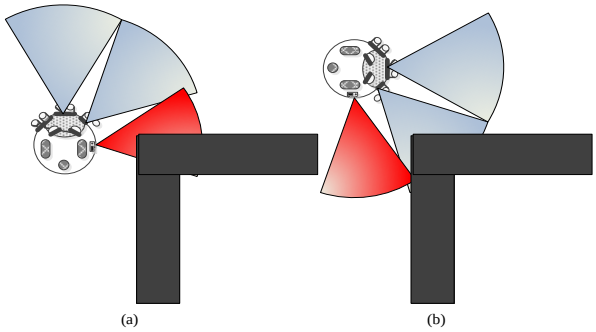

Fig. 13. Second situation. The sharp corner appears in two situations: (a) handled by rules 21, 22, 24 &25; (b) handled by rules 13~15 (with reference to Table 2 and Table 3).

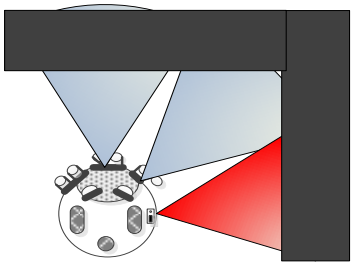

Fig. 14. Third situation. The mobile robot faces a convex corner (i.e. wall segments from both walls of a corner are sensed) (with reference to Table 3)

Table 3. Rules for tackling commonly encountered situations of right wall following

Situation	Applicable Rules
The first situation (flat wall) Fig.12	
(a)	11~15
(b)	1~10
(c)	Left Rotation
(d)	16~23
(e)	24, 25
(f)	24, 25
The second situation (sharp corner) Fig. 13	
(a)	21, 22, 24, 25
(b)	13~15
The third situation (deadend) Fig. 14	
Rotation on the spot counterclockwise	

In these figures, there are three scan ranges: the blue scan light represents sonar, while the red scan light represents the IR sensor. The second (ii) and third (iii) situations we consider are when the mobile robot perceives a corner from outside and inside, respectively. In the former situation (ii) of outside the corner, it is possible that the mobile robot loses sensing of the corner if it is moving too fast or if the corner is too far away from the mobile robot. To turn around a corner with orientation discontinuity along the wall from outside, the corner is within the fields of view (linear and angular sensing ranges) of the range sensors for all instants of time.

Now we present the intelligence of the wall-following system summarized in Table 3 based on sensor readings, i.e.

perception and action of the mobile robot in executing the task of wall following based on Table 2, for the determination of heading angle in the aforementioned three situations. The first situation is that only one wall is sensed and this could appear in six situations for the design of the rule base, which are shown in Fig. 12. In Fig. 12(a), both the front right and the right sensors detect a medium distance to the wall, and the mobile robot moves along the wall. As to the situation depicted in Fig. 12(b) in which the mobile robot is too close to the wall, we can see that rules 1 to 10 of Table 2 in which the robot turns very left or normal left are applicable. Once the front sensing detects a safe distance like that in situation Fig. 12(c), the mobile robot turns to the left. At the same time, the mobile robot must turn right to find a right wall when it meets the situations of Fig. 12(d), (e) and (f).

The second situation is to traverse around the sharp corner shown in Fig. 13 safely. Two decision situations are encountered. Formally, suppose a global coordinate frame is set to define one wall with the equation $w_a(x, y) = 0$ and the other wall with the equation of the corner as $w_b(x, y) = 0$ in Fig. 13. Suppose we are given two positions: the current robot position (x_a, y_a) in the situation shown in Fig. 13(a) and the robot position (x_b, y_b) after a right (clockwise) turn in the situation shown in Fig. 13(b). Then whenever

$$w_a(x_a, y_a)w_a(x_b, y_b) < 0$$

and

$$w_b(x_a, y_a)w_b(x_b, y_b) < 0$$

both hold, we see that the robot has turned around the corner and detects a new wall of the corner to be followed by the robot. Note that since constant path velocity v is maintained during cornering, the acceleration of turning around the corner has only normal component given by $a = \kappa v^2$, where κ is the curvature of turning defined in (1) .

To implement this cornering process, firstly the situation of Fig. 13(a) is that the mobile robot moves parallel to the right wall until it enters an empty space where front right sensors cannot detect the wall but right sensors detect the wall. This is identified as the robot passing over a discontinuity of curvature or an irregularity where abrupt variation of sensor readings is observed, i.e. the vertex of the corner. In this situation, Rules 21, 22, 24 and 25 in Table 2 handle this situation, and the decision for action is a right turn. As the robot has already passed over the vertex of the corner and made a right turn subsequently, it detects a right wall (the other wall on its right) again as depicted in Fig. 13(b). It is handled by rules 13~15, in which the desired motion is right wall following.

The third situation is shown in Fig. 14 [16, 32] in which the robot has entered into a convex corner (perceived as a dead end) as the robot senses two walls, for which the front sensor also has readings, in addition to the right-side sensors. When this situation occurs, the action taken by the robot is a rotation on the spot to reorient the robot until there are no readings in its front sensor, then it switches to the first and second situations.

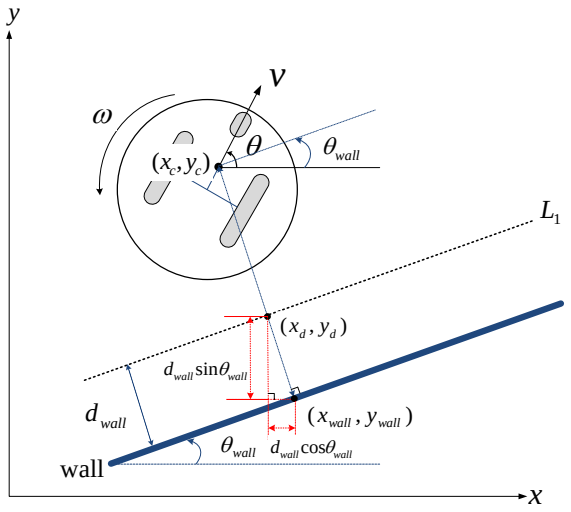

Fig. 15. The figure showing the wall-following kinematics in the inertial frame, where (x_d, y_d) and (x_{wall}, y_{wall}) are the projections of point (x_c, y_c) on L_1 and the wall, respectively.

Event-based Practical Stability Analysis

Wall Following Kinematics

In general, wall following can be viewed as a variation of path following [36] from control design of view, where the path is a virtual line parallel to the wall. The unicycle (1) is a small time controllable system everywhere [47], so that there exists a collision-free motion to reach a configuration $(x(t_{i+1}), y(t_{i+1}), \theta(t_{i+1}))$ at $t = t_{i+1}$ in a neighbourhood Ω of any configuration $(x(t_i), y(t_i), \theta(t_i))$ at $t = t_i$ within a finite time using control of linear (constant in this paper) and angular velocities.

Now refer to Fig. 15. Consider a representative point (x_c, y_c) of the robot (the center of mass, subscript *c*, is omitted in the following expressions) and let (x_d, y_d) and (x_{wall}, y_{wall}) be the orthogonal projection of point (x_c, y_c) onto the virtual corridor line L_1

$$L_1 = \{(x - x_{wall})\sin\theta_{wall} - (y - y_{wall})\cos\theta_{wall} = 0\}$$

to be followed by the mobile robot at a distance

$$d_{wall} = (x_d(t) - x_{wall}(t))\sin\theta_{wall} - (y_d(t) - y_w(t))\cos\theta_{wall}.$$

Then

$$\tilde{x}(t) = ((x_c - x_{wall})^2 + (y_c - y_{wall})^2)^{1/2} - d_{wall}$$

represents the deviation of the robot from the desired virtual corridor line L_1 at any time t. Define

$$\varphi(t) = \theta(t) - \theta_{wall}$$

to represent angular deviation as related to the virtual corridor axis.

The kinematics of path following can be derived [36, 32] as

$$\begin{pmatrix} \dot{\tilde{x}} \\ \dot{\varphi} \end{pmatrix} = \mathbf{f}(\tilde{x}, \varphi, v, \omega) = \begin{pmatrix} v \sin\varphi \\ \omega \end{pmatrix}. \quad (19)$$

where the robot state is expressed in terms of distance and orientation relative to the line L_1. The vector field $\mathbf{f}(\tilde{x}, \varphi, v, \omega)$ is Lipschitz in state with $\mathbf{f}(0,0,0,0) = 0$, and there is no finite escape if the state feedback control (v, ω) is continuously differentiable. Furthermore, for zero input, any state $(\tilde{x}, \varphi)$ is an equilibrium point. [33] observed that wall following behaviour corresponding to $(\tilde{x}, \varphi) = (0,0)$ is a stable equilibrium of wall-following dynamics. Thus, the objective of navigation is the convergence of state to the origin $(\tilde{x}, \varphi) = (0,0)$, i.e. navigation of the mobile robot to the line L_1 that is parallel to the wall at a distance d_{wall}.

In practice, the state φ can be estimated [33], e.g. from the fusion and Kalman filtering of a collection of sensor readings over multiple measurements [4, 32] or from the average of an equation derived from trigonometry of sensor readings of front, front right and right sensors within the sensing ranges [15]. The state $(\tilde{x}, \varphi)$ can thus be derived from raw sensor readings [42] as

$$\tilde{x} = \frac{d_{frw}(t) + d_{rw}(t)}{2} \cos\varphi$$
$$\cos\varphi = \frac{\left| d_{frw}(t) - d_{rw}(t) \right|}{\sqrt{L_s^2 + (d_{frw}(t) - d_{rw}(t))^2}} \quad (20)$$

where L_s is the distance between front right and right sensors, $d_{frw}(t), d_{rw}(t)$ are the sensor readings of front right and right sensors, respectively, to the wall at time *t*. It can be seen that if $d_{frw}(t) \approx d_{rw}(t)$, then $\varphi \approx 0$. If further $d_{frw}(t) \approx d_{rw}(t) \approx d_{wall}$, then $\tilde{x} \approx 0$.

For the wall-following kinematics (19), for a constant v, [36, 32] constructed a common Lyapunov function and the design of smooth angular velocity controller $\omega = \omega(\tilde{x}, \varphi)$ with $\omega(0,0) = 0$ based on the class K function. [32] proposed the stable switching of three behaviors (wall following, circle following, and rotation on the spot [1], with each described by a differential or an algebraic equation) based on a supervisor logic for wall following control. [34] proposed a stable navigation law for border patrolling by a constant-speed unicycle (1), assuming that only range measurements and its derivatives $\tilde{x}, \dot{\tilde{x}}$ are available so that $\tilde{x}, \varphi \to 0$ as $\tilde{x}, \dot{\tilde{x}} \to 0$. The dynamical-system approaches to wall following [4], [7], [32], [34] required that perfect measurements of the state be available at each time instant to achieve asymptotic convergence of path-following errors to zero. However, the actual behaviors of reactive wall following depend on the sensor configurations, the sensor types, and the resolution and sensing range of each sensor, since the platform contains uncertain parameters and unmodelled bounded disturbances, and the measurement and the action also contain uncertainty that causes the robot to accumulate localization errors while following the wall. In the presence of heading errors, uncertainties in sensor feedback and thus the wall, or equivalently uncertainty in estimation of the robot state $(\tilde{x}, \varphi)$ of (19), we restrict ourselves to show the practical stability in the following, i.e. stabilization to a prescribed neighborhood of the origin, instead of Lyapunov stability.

Event-based Analysis of Practical Stability

Wall following is a reactive behavior [1] that allows event-based analysis via finite-state machine or automaton [44] without explicit control expressions. Here, for our working rule-based reactive navigation system, the navigation is a finite series of actions taken by the robot at the event times, and an action implemented by the interval type-2 fuzzy control is taken by the robot only when a rule is activated based on online sensor readings. This is suited to invoking the behavior reasoning and computation framework of event-based control [44] for event-based practical stability analysis with respect to a domain of initial and subsequent deviation of wall following error over a time interval in the following subsection. Note further that the mathematical model of a unicycle (1) is controllable and thus the unicycle can realize any desired path required by the rules, so that the behaviors are kinematically feasible and reactive.

Our event-based practical stability analysis that follows is based on raw sensor readings of right and front right sensors to get an intuitive justification of how the robot reacts in each encountered situation in a qualitative sense without constructive mathematical details of how the robot motion continuously evolves. As indicated by the rules of Table 2, the sensor readings d_{frw}, d_{rw} of front right and right sensors are two independent inputs during right-wall following, while the uncertainties are better handled by the type-2 fuzzy system for enhancing the performance of navigation. The perception-action mapping defines a nonlinear affine input-state system (19) without drift term via the rule tables.

Firstly, the rules guarantee that the robot could successfully turn around the sharp corner or deadend shown in situation 2 and situation 3 depicted in Fig. 13 and Fig. 14, and the loss of wall can be recovered via applying rules 24 and 25, which tackle the situation in which the robot is far from the wall. It

may take a long settling time for the robot to reach the wall-following mode. Let $t = t_0$ denote the start of robot forward motion. Denote by $\{t_i, i = 1,2,\cdots\}$ the times that the robot takes $\sigma(t_i) \in \{1,2,\cdots\}$ th (possibly the same as previous) action recommended by the fuzzy rule base according to the sensor readings, which lasts over the duration $[t_i, t_{i+1})$ between two consecutive actions that we do not know in advance. The time t_i is determined online according to the sensor readings that continuously monitor the state (distance and orientation to the virtual line) of the robot. it is therefore of interest to show that the robot state is guaranteed to converge to a set Ω representing a specified tolerance (neighborhood) of the origin in all situations shown in Fig. 12 within a time interval $[t_i, t_{i+1})$. That is, the robot could recover from the deviation from parallelism to the wall caused by the localization error and measurement uncertainties once it is in the wall-following mode.

In the sequel, we use the notation $X \approx_{\varepsilon} Y$ to denote $|X - Y| \le \varepsilon$, i.e. $Y - \varepsilon \le X \le Y + \varepsilon$ for any two numbers X, Y that are close enough within a given tolerance ε , where ε can be arbitrarily small.

Now suppose at an event time t_i , the robot does not follow the parallel to the wall (i.e. the front right sensor reading is not at medium). In practice, this is expressed as $|\varphi(t_i)| > \varepsilon$ for a threshold ε . Then, either it is to be in collision with the wall it is required to follow currently, or it is away from the wall. In either case, we argue that based on iteratively approaching the virtual line L_1 by at least some increment in a successive finite time intervals via the series of actions taken by the robot according to the fuzzy rules, render that whenever $|\varphi(t_i)| > \varepsilon$ occurs, the state of the reactive system over a time interval is such that $|\varphi(t_{i+1})| < |\varphi(t_i)|$ or $|\varphi(t_{i+1})| \approx |\varphi(t_i)| \approx_{\varepsilon} 0$, where t_{i+1} is the time of another action. Then $\{|\varphi(t_i)|\}$ is either below ε or a positive and decreasing sequence regulated to a value below ε , and the desired safety distance d_{wall} (set as medium in the membership function) to the wall is maintained within a threshold d_{th} .

In general, wall following is performed by first steering the robot to approach the virtual line L_1 , and then moves along L_1 . We assume that there exists a nominal navigation $(v^0(t), \omega^0(t)), t \in [0, t_0)$ [34] to drive the robot to a proper initial state $(x(t_0), y(t_0), \theta(t_0)) \in \Omega$ [1] after a transient so that at $t = t_0$, the start motion is forward with constant speed v and the initial heading is such that readings of both right and front right sensors are medium or near. As the robot state is within Ω , the interval type-2 fuzzy control is aimed to stabilize the robot with respect to L_1 by enhancing the robustness to small wall following errors around the line L_1 . From the relation of (20), it is seen that

$$d_{frw} \approx d_{rw} \Rightarrow \varphi \approx_{\varepsilon} 0 .$$

And if further

$$d_{frw} \approx d_{rw} \approx_{d_{th}} d_{wall} \Rightarrow \varphi \approx_{\varepsilon} 0, \tilde{x} \approx_{d_{th}} 0$$

where ε, d_{th} are the user-defined tolerable linear and angular accuracy of navigation, respectively.

Denote by Ω the constraint set of configurations such that the mobile robot is at the following mode defined by the notion of "moving and keeping perception constant" [43]:

$$\Omega = \{(x, y, \theta) : d_{frw} \approx d_{rw} \approx_{d_{th}} d_{wall}(\text{medium})\} \tag{22}$$

where linearization of (19) is representative of the wall-following behavior.

Remark. Alternatively, according to the treatment of [40], the state constraint set

$$\Omega = \{(x, y, \theta) : \|(x, y) - (x_d, y_d)\| \le d_{th}, |\varphi| \le \varepsilon\}$$

defines the upper bound of the deviation from the virtual (or nominal) system kinematics moving on L_1

$$\begin{cases} \dot{x}_d = v_d \cos\theta_{wall} \\ \dot{y}_d = v_d \sin\theta_{wall} \\ \dot{\theta}_{wall} = \omega_{wall} \end{cases} \tag{23}$$

Without loss of generality, the mobile robot is assumed to operate in a region Ω of the configuration space initially at $t = t_0$. According to the partition of front right sensing range, the tendency of behaviors in each situation depicted in Fig. 12, after execution of an activated rule at $t = t_i$ (viewed as an event that happened at $t = t_i$) over an a priori unknown interval $[t_i, t_{i+1})$, is analyzed as follows.

(si) The nominal right-wall following at $t = t_i$ is shown in Fig. 12(a), for which rules 11~15 are applicable. In this case, $d_{frw_j}(t_i)$ is medium ($\approx d_{wall}$) and commanded heading is medium (around 0^0), so that the tendency is to align the robot with the virtual line L_1 :

$$d_{frw}(t_{i+1}) \approx d_{frw}(t_i),$$
$$d_{rw}(t_{i+1}) \approx_{d_{th}} d_{wall},$$

$$|\varphi(t_{i+1})| \approx |\varphi(t_i)| \approx_{\varepsilon} 0$$

(sii) To be in collision with the wall at $t = t_i$ as shown in Fig. 12(b), rules 1~10 are applicable. In this case, $d_{frw}(t_i)$ is near and very near, and the commanded heading is left, so that after executing each rule

$$d_{frw}(t_{i+1}) > d_{frw}(t_i),$$
$$d_{rw}(t_{i+1}) > d_{rw}(t_i),$$
$$|\varphi(t_{i+1})| < |\varphi(t_i)|$$

Repeatedly applying rules 1~10 whenever appropriate, the tendency of successive movements is that $d_{frw}(t_{i+M})$ is medium after applying a finite number *M* of rules. We come to the nominal situation **(si)** again.

(siii) The robot is to be in collision with the wall as shown in Fig. 12(c) at $t = t_i$, $|\varphi(t_i)| \approx_{\varepsilon} \pi/2$ and that $|\varphi(t_{i+1})| < |\varphi(t_i)|$ after the execution of the action that commanded heading is left. Then we may come to the situation **(sii)** above.

(siv) The robot is away from the wall at $t = t_i$: this includes Fig. 12(d), for which rules 16~23 are applicable, together with Fig. 12(e) and (f), for which rules 24~25 are applicable. In this situation, $d_{frw}(t_i)$ is far and very far, the commanded heading is right or medium, which yields $d_{rw} \approx_{d_{th}} d_{wall}$, or $d_{frw}(t_{i+1}) < d_{frw}(t_i)$. Repeatedly applying rules 16~25 whenever appropriate, we see that ultimately $d_{frw}(t_{i+N})$ will be getting closer to d_{wall} or be decreasing after a finite number *N* of consecutive applications, so that either

(si) the nominal situation $d_{rw} \approx_{d_{th}} d_{wall}, |\varphi(t_{i+N})| \approx_{\varepsilon} 0$, or

(sii) the potential collision situation $d_{frw}(t_i)$ is near, or

(siii) $|\varphi(t_{i+Ni})| \approx \pi/2$

mentioned above occurs.

The aforementioned event-based arguments have focused on the qualitative and inductive verification of stable wall following in the context of input-state stability of (19) via inferring in an intuitive way. As a result of the above qualitative behavior analysis, there exists a region of attraction in configuration space for (1) where all start motions of (19) converge to a stable wall following using fuzzy reactive behaviors in the state-action space defined by the perception-action mapping. We will see in our experiments that this event-based analysis is a good approximation to the stable wall-following behaviors in practice.

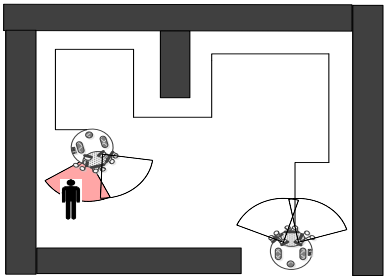

Fig. 16. A practical surveillance scenario using a mobile robot based on wall following that online detects and responds to the presence of a human on the wall-following route. The wall has concave and convex parts. The red scan light denotes detecting an invader while the robot keeps moving along the right wall, and due to security concerns, the mobile robot will sound an alarm and capture real-time images and videos of human activity.

Experimental results and discussions

The variation of interval type-2 fuzzy controller is employed in the real mobile robot experiments conducted in indoor environments. We will describe in this section two indoor right-wall following experiments, one on a corridor and the other on complex polygon terrain. The navigation system is verified to exhibit behaviors that correctly react to the commonly encountered situations and achieve stable wall following in practice.

Experimental setup

An experimental testing scenario of invader detection during the execution of the wall following is designed as shown in Fig. 16. Whenever a person appears on the wall-following path, in general the trajectory (i.e. motion model) of the person need to be estimated based on the intentions of the person for safe navigation of the mobile robot [46]. In this work, to minimize the risk of collision with the person on the wall following route detected instantly by using human detection sensors, for the purpose of surveillance, the robot temporarily stops its motion at the cost of longer duration of wall following, sounds security alarms, takes a photo and sends it to inform the remote user, then keeps moving forward using wall following after the human leaves. The event of human appearance can thus be well handled by the reactive wall following. In this scenario, the mobile robot moves at a constant linear velocity in an unknown indoor environment according to the flow chart of Fig. 17 using right-wall following and human detection. In the following, we demonstrate that the surveillance system works properly using stable human-aware wall following in the real world. The experiments were conducted in two types of environment: a corridor and complex polygon terrain. The initial configuration of the mobile robot is in alignment with the virtual line L_1, and the wall following control is activated from the start of robot motion.

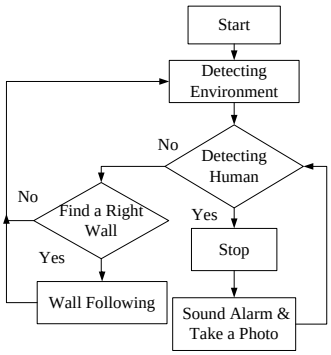

Fig. 17. The flow chart of a practical surveillance system integrating wall following with continuous human detection in which the mobile robot follows a wall by keeping the wall to its right. The human detection sensors are in charge of detecting the presence of human. The robot stops at the detected human, sounds an alarm and takes a photo of human, and waits until the human leaves.

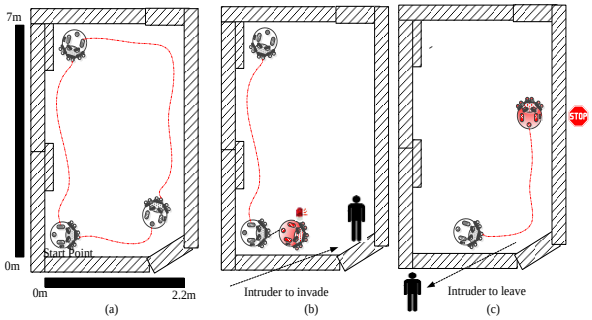

Fig. 18. Experiment 1: right-wall following with human detection in a corridor (a) The map and the wall-following route (red dash-dot-dot line). (b) Detecting the appearance of an invader who stands in the wall-following route. (c) The robot continues its wall-following motion in a corridor in which the red stop sign denotes the checkpoint that the stop command.is activated.

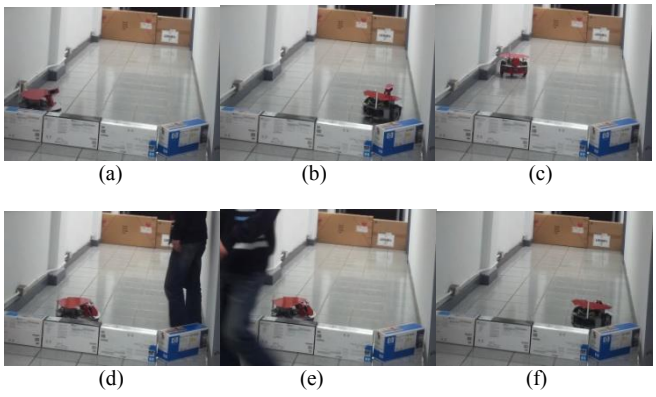

Fig. 19. Snapshots of experiment 1 demonstrating intelligent human-aware wall following in a corridor.

Experimental results

Experiment 1: Experiment on a corridor

We perform an experiment on a corridor environment to perform the task of surveillance, and the detection of an intruder. Initially, the mobile robot was placed at the lower left corner of the test environment with its orientation toward the right. Fig. 18(a) shows the route of the wall following in a corridor. Due to errors in orientation, the robot does not travel exactly parallel to the wall. The mobile robot detects an invader when wall following proceeds on a second lap, and the mobile robot sounds a security alarm and takes a photo, as shown in Fig. 18(b). The mobile robot continues to perform the wall-following task as the invader walks away and stops whenever it meets the stop command, as shown in Fig. 18(c).Snapshots of this navigation experiment are shown in Fig. 19. The velocity values of the left and right wheels of the mobile robot for this navigation experiment are shown in Fig. 20. The negative left wheel velocity denotes forward rotation, while the right wheel velocity denotes backward rotation. The human detection sensor feeds back a voltage to the mobile robot, and we can see from Fig. 21 that when the amplitude of the voltage exhibits a strong shock (red line) and lasts over about 60~70s of time, it reflects the heat radiated by the human during the human appearance.

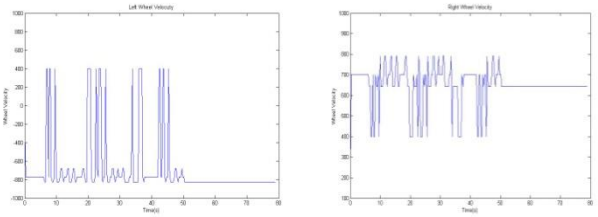

(a) Left wheel speed (b) Right wheel speed

Fig. 20. Wheel velocities as inputs to the mobile robot that moves in constant translational speed while the heading is controlled by an interval type-2 fuzzy control in experiment 1.

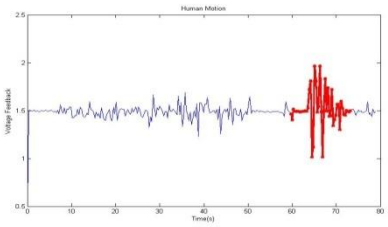

Fig. 21. Human detection sensor voltage feedback to mobile robot in experiment 1

Experiment 2: Experiment on complex polygon terrain

We perform another experiment involving surveillance on complex polygon terrain. In this scenario, initially the mobile robot was placed at the upper right corner near the door of the test environment with its orientation toward the left. The resulting trajectory of navigation is shown in Fig. 22(a). The mobile robot performs wall following and passes around the small cusp without entering it due to maximal curvature constraint $\kappa_{max} = \omega_{max}/v$. It detects an invader opening a door, and the mobile robot sounds a security alarm as shown in Fig. 22(b). The mobile robot continues to perform its patrol in the wall-following task when the invader leaves until it meets a stop command, as shown in Fig. 22(c). This experiment is shown in the snapshots of Fig. 23, with the wheel velocities shown in Fig. 24. The strong shock voltage of the human detection sensor shown in the red line of Fig. 25 indicates the appearance of a person in the wall-following route, as shown in the snapshot of Fig. 23(d). The motion

control is powered by a DC motor battery and a DSP board, and their energy consumption is shown in Fig. 26.

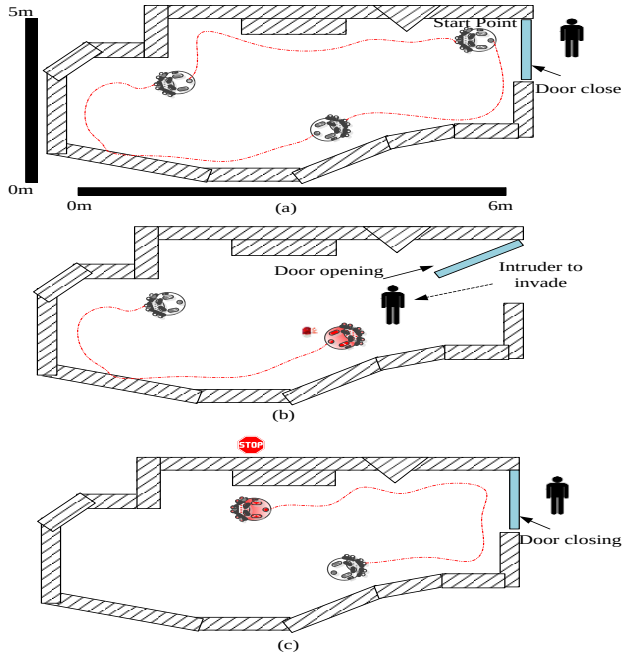

Fig. 22. Experiment 2: right-wall following with human detection on complex polygon terrain. (a) The map and the wall-following route (red dash-dot-dot line) (b) Detecting the appearance of an invader. (c) The robot continues its wall-following motion on complex polygon terrain in which the red stop sign denotes the checkpoint that the stop command .is activated.

Discussions

(i)Reactivity is important in unknown environment since it allows the faster response. The reactivity of a wall following mobile robot is revealed in the experiments. The reactivity is state-dependent and event-based, with the human detection sensors the robot is capable of restart of wall following whenever an early detection of human appears in the route that causes the temporary stop of robot and walks away.

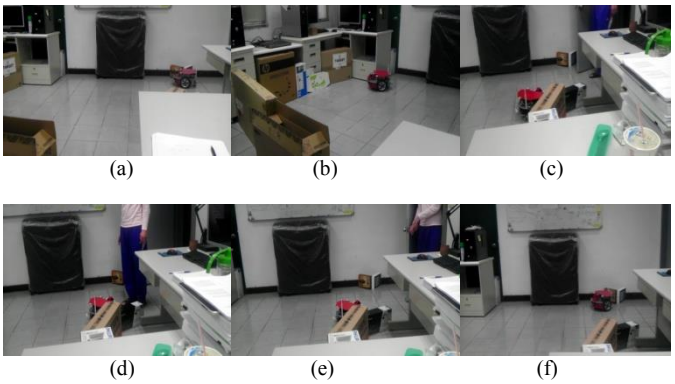

Fig. 23. Snapshots of experiment 2 demonstrating intelligent human-aware wall following on complex polygon terrain

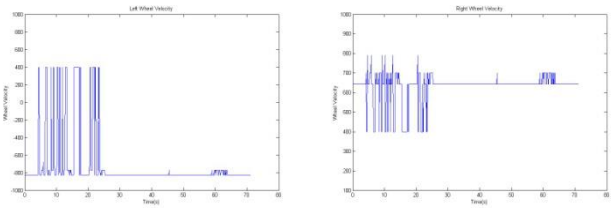

Fig. 24. Wheel velocities as inputs to the mobile robot that moves in constant translational speed while the heading is controlled by an interval type-2 fuzzy control in experiment 1.

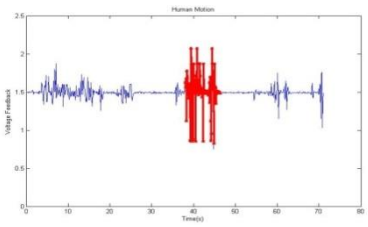

Fig. 25. Human detection sensor voltage feedback to mobile robot in experiment 2

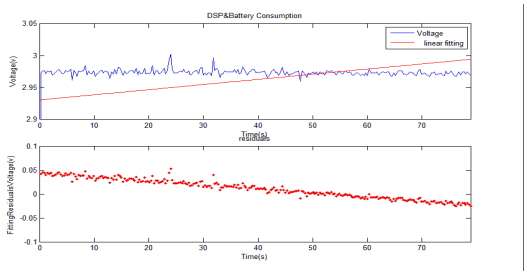

Fig. 26 DSP board and DC motors battery consumption in experiment 2

(ii) From the experimental results, the sensors assist the robot to correctly detect the walls and humans it faces in a closed indoor environment. The robot kept a constant speed and followed the wall at most travelling time, while it deviated the most from the wall around the corners that require significant vehicle heading change to bypass the concave or convex parts in a stable manner, stops before the detected human, and it again continues the wall-following task as the human walks away and disappears (as indicated by Fig. 19(d) and (e) for experiment 1 and Fig. 23 (d) and (e) for experiment 2). In both experiments, cornering induces the worst deviation in distance during wall following. We see that as the mobile robot got too closer to the wall $((\tilde{x},\varphi)\notin\Omega,\tilde{x}<0)$, the wall following control could effectively correct the discrepancy so that the robot recovers rapidly to the region Ω of practical stability.

(iii)Since the navigation is smoother using an interval type-2 fuzzy differential velocity control approach, the system is more economical in the spirit of energy management [2] as well as the reduction of vibration caused by smooth navigation. These features increase the stability, comfort and safety of navigation behaviours required by a robotic wheelchair at low cost in order to prevent wall collisions when

a user manually or semi-autonomously steers a battery-powered wheelchair in a corridor using wall following for a long time.

(iv)It is remarked that all the sensing, computations and decision making can be done in real time for reactive wall following due to the simplicity and computational efficiency of the fuzzy system described by the rules and the inferred perception-action mapping for wall following, and only one action derived from a rule is activated. However, in complex environment, fusion of multiple behaviors and larger size and complex rule tables must be devised or learned. In our experiments, only one human is detected at a time, and multiple humans could be detected if each appears separately at different time intervals.

Conclusions

For the particular application of autonomous mobile robot navigation to indoor surveillance, the requirements are the ability to react to emergent situations and to be energy-saving. This paper demonstrates an autonomous indoor surveillance system. The system we are working on is a commercially available wheeled mobile robot platform equipped with range and human detection sensors. We take advantage of reactive wall-following behavior that allows the proper reaction to unexpected human presence, while dealing with the uncertainties and constraints of real-time navigation based on a two-input (distances) single-output (heading angle) interval type-2 fuzzy logic system. The kinematic wall-following mobile robot is demonstrated to be stable and safe for accomplishing the task of surveillance in real unknown indoor environments. Moreover, the system could be used to capture real-time images and videos during patrolling to assist human surveillance, where the human face detection of an unknown human is undertaken by the remote user. This functionality of human face detection could be carried out more automatically with the use of existing face detection software [11].

REFERENCES

[1] Ando Y., Tsubouchi T., & Yuta S.. A reactive wall following algorithm and its behavior of an autonomous mobile robot with sonar ring. *Journal of Robotics and Mechatronics* 1996; **8**:33-39.

[2] Barili A., Ceresa M., & Parisi C.. Energy-saving motion control for an autonomous mobile robot. *IEEE International Symposium on Industrial Electronics* 1995: 674-676.

[3] Barshan B.. Accurate profile extraction and mapping by intelligent processing of ultrasonic range data. *Electronics Letters* 2007; **43**(24):1396-1398.

[4].Bemporacl A, Di Marco M., & Tesi A.. Sonar-based wall-following control of mobile robots. *ASME Journal of Dynamic Systems, Measurement and Control* 2000;**122**(1): 226-230.

[5] Borenstein J. & Koren Y.. Obstacle avoidance with ultrasonic sensors. *IEEE Journal of Robotics and Automation* 1998;4(2): 213-218.

[6] Bortot D., Hawe B., Schmidt S., & Bengler K.. Industrial Robots-The new friends of an aging workforce. *Advances in Ergonomics in Manufacturing* 2013:253-262.

[7] Carelli R. & Freire E. O.. Corridor navigation and wall-following stable control for sonar-based mobile robots. *Robotics and Autonomous Systems* 2003;**45**(3):235-247.

[8] Castillo O. & Melin P.. A review on interval type-2 fuzzy logic applications in intelligent control. *Information Sciences* 2014;**279**: 615-631.

[9] Lopez de Mantaras R. and Lopez-Sanchez M. Adding reactivity to path following by an autonomous robot. *7th IEEE International Conference on Emerging Technologies and Factory Automation* 1999: 1501-1510.

[10] Choi B., Meriçli C., Biswas J. & Veloso M.. Fast human detection for indoor mobile robots using depth images. *IEEE International Conference on Robotics and Automation* 2013:1108-1113.

[11] Correa M., Hermosilla G., Verschae R., & Ruiz-del-Solar J.. Human detection and identification by robots using thermal and visual information in domestic environments. *Journal of Intelligent & Robotic Systems* 2012;**66**(1-2): 223-243.

[12] Curiac D. I., & Volosencu C.. A 2D chaotic path planning for mobile robots accomplishing boundary surveillance missions in adversarial conditions. *Communications in Nonlinear Science and Numerical Simulation* 2014;**19**(10):3617-3627.

[13] De A. & Koditschek D. E.. Toward dynamical sensor management for reactive wall-following. *IEEE International Conference on Robotics and Automation* 2013: 2400-2406.

[14]Dr. Robot Inc. DHM5150 Human motion sensor user manual (http://www.drrobot.com/products/item_downloads/DHM5150_1.pdf) 2005.

[15] Hsu C. H. & Juang C. F.. Evolutionary robot wall-following control using type-2 fuzzy controller with species-DE-activated continuous ACO. *IEEE Transactions on Fuzzy Systems* 2013;**21**(1):100-112.

[16] Huang L.. Wall-following control of an infrared sensors guided wheeled mobile robot. *International Journal of Intelligent Systems Technologies and Applications* 2009;**7**(1):106-117.

[17] Jing X. J.. Behavior dynamics based motion planning of mobile robots in uncertain dynamic environments. *Robotics and Autonomous Systems* 2005;**53**(2):99-123.

[18] Kruse T., Pandey A. K., Alami, R., &. Kirsch A. Human-aware robot navigation: A survey. *Robotics and Autonomous Systems* 2013;**61**(12):1726-1743.

[19] Lamperski A. G., Loh O. Y., Kutscher B. L., & Cowan N.J.. Dynamical wall following for a wheeled robot using a passive tactile sensor. *IEEE International Conference on Robotics and Automation* 2005:3838-3843.

[20] Ray A. K., Behera L., & Jamshidi M. . Sonar-based rover navigation for single or multiple platforms: forward safe path and

target switching approach. *IEEE Systems Journal* 2008; *2*(2),:258-272.

[21] Lo C. W., Wu K. L., Lin Y. C., & Liu J. S.. An intelligent control system for mobile robot navigation tasks in surveillance. In *Robot Intelligence Technology and Applications* 2 2014: 449-462.

[22] Mendel J., Hagras H., Tan W. W., Melek W. W., & Ying H..*Introduction to Type-2 Fuzzy Logic Control: Theory and Applications*:John Wiley & Sons, 2014.

[23] Moreno L., Armingol J. M., Garrido S., De La Escalera A., & Salichs M. A.. A genetic algorithm for mobile robot localization using ultrasonic sensors. *Journal of Intelligent and Robotic Systems* 2002;**34**(2):135-154.

[24] Najmaei N., Kermani M. R., & Al-Lawati M. A.. A new sensory system for modeling and tracking humans within industrial work cells. *IEEE Transactions on Instrumentation and Measurement* 2011;**60**(4):1227-1236.

[25] Ollero A., García-Cerezo A., Martínez J. L., & Mandow A.. Fuzzy tracking methods for mobile robots. In M. Jamshidi ed., *Applications of Fuzzy Logic: Towards high machine intelligence quotient systems* 1997: 347-364.

[26] Sun T., Pei H., Pan Y., & Zhang C.. Robust adaptive neural network control for environmental boundary tracking by mobile robots. *International Journal of Robust and Nonlinear Control* 2013;**23**(2):123-136.

[27] Tsui W., Masmoudi M. S., Karray F., Song I., & Masmoudi. M. Soft-computing-based embedded design of an intelligent wall/lane-following vehicle. *IEEE/ASME Transactions on Mechatronics* 2008;**13**(1):125-135.

[28] Van Turennout P., Honderd G., & Van Schelven L. J.. Wall-following control of a mobile robot. *IEEE International Conference on Robotics and Automation* 1992:280-285.

[29] Yata T., Kleeman L., & Yuta S. I.. Wall following using angle information measured by a single ultrasonic transducer. *IEEE International Conference on Robotics and Automation* 1998:1590-1596.

[30] Yun X., & Tan K. C .. A wall-following method for escaping local minima in potential field based motion planning. *8th International Conference on Advanced Robotics* 1997: 421-426.

[31] Heidari F., & Fotouhi R.. A human-inspired method for point-to-point and path-following navigation of mobile robots. *ASME Journal of Mechanisms and Robotics* 2015;7(4):18 pages.

[32] Toibero J. M., Roberti F., & Carelli R.. Stable contour-following control of wheeled mobile robots. *Robotica* 2009;**27**(1):1-12.

[33] Bicho E.. Detecting, representing and following walls based on low-level distance sensors. *Second International ICSC Symposium on Neural Computation* 2000.

[34] Wang C., Matveev A. S., Savkin A. V. & Hoy M.. *Safe Robot Navigation among Moving and Steady Obstacles*: Elsevier, 2015.

[35] Do K. D.. Global output-feedback path-following control of unicycle-type mobile robots: A level curve approach. *Robotics and Autonomous Systems* 2015;**74**:229-242.

[36] Samson, C. . Path following and time-varying feedback stabilization of a wheeled mobile robot.*IEEE International Conference on Advanced Robotics and Computer Vision 1* 1992:1.1-1.5, 1992.

[37] Defoort M., Palos J., Kokosy A., Floquet T., & Perruquetti W.. Performance-based reactive navigation for non-holonomic mobile robots. *Robotica* 2009;**27**(2):281-290.

[38] Thrun S., Burgard W., & Fox D.. *Probabilistic robotics*. 2005, MIT Press.

[39] Dash T.. Automatic navigation of wall following mobile robot using Adaptive Resonance Theory of Type-1. *Biologically Inspired Cognitive Architectures* 2015;**12**: 1-8

[40] Chung T. L., Bui T. H., Kim S. B., Oh M. S., & Nguyen T. T.. Wall-following control of a two-wheeled mobile robot. *KSME International Journal* 2004;**18**(8):1288-1296.

[41] Libal, U., & Płaskonka, J. . Noise sensitivity of selected kinematic path following controllers for a unicycle. *Bulletin of the Polish Academy of Sciences: Technical Sciences* 2014; ***62***(1): 3-13.

[42] Hanafi D., Abueejela Y. M., & Zakaria M. F.. Wall follower autonomous robot development applying fuzzy incremental controller. *Intelligent Control and Automation* 2013;**4**(1):18-25.

[43] Braunsting R. & Ollero A.. Evaluating the wall following behaviour of a mobile robot with fuzzy logic. *IFAC/IMACS International Workshop on Artificial Intelligence in Real Time Control* 1995: 89-93.

[44]Rigatos G.. Models of computation for reactive control of autonomous mobile robots. *Expert Systems with Applications* 2012;**39**(8):6767-6773.

[45] Dong, J. F., Sabastian, S. E., Lim, T. M., & Li, Y. P.. Autonomous in-door vehicles. *Handbook of Manufacturing Engineering and Technology*:Springer London,2015, 2301-2346.

[46]Arndt, M., & Berns, K.. Safe predictive mobile robot navigation in aware environments. *12th International Conference on Informatics in Control, Automation and Robotics (ICINCO)*,2015,Vol. 2: 15-23.

[47] Laumond, J. P., Sekhavat, S., & Lamiraux, F.. Guidelines in nonholonomic motion planning for mobile robots. *Robot motion planning and control*, 1998:1-53.